Conf-910602--38



# SEISMIC RESPONSE ANALYSES OF BASE ISOLATED STRUCTURES WITH HIGH DAMPING ELASTOMERIC BEARINGS

by



C. Y. Wang, Y. Tang, A. H. Marchertas,* Y. W. Chang, and R. W. Seidensticker

Reactor Engineering Division
Argonne National Laboratory
Argonne, Illinois 60439, U.S.A.

ANL/CP--72573

DE91 011843

## ABSTRACT

Seismic response analysis of base-isolated structures with high damping elastomeric bearings is described. Emphasis is placed on the adaptation of a nonlinear constitutive model for the isolation bearing together with the treatment of foundation embedment for the soil-structure-interaction analysis. The constitutive model requires six input parameters derived from bearing experimental data under sinusoidal loading. The characteristic behavior of bearing, such as the variation of shear modulus and material damping with the change of maximum shear deformation, can be captured closely by the formulation. In the treatment of soil embedment a spring method is utilized to evaluate the foundation input motion as well as soil stiffness and damping. The above features have been incorporated into a three-dimensional system response program, SISEC, developed at Argonne National Laboratory. Sample problems are presented to illustrate the relative response of isolated and unisolated structures.

---

*Northern Illinois University, DeKalb, Illinois 60015.

## DISCLAIMER

## INTRODUCTION

Seismic base isolation is certainly one of the most significant earthquake engineering innovations in recent years [1] due to its significant capability of protecting structures from earthquake damage. One main concept in base isolation is to reduce the fundamental frequency of structural vibration to a value lower then the energy-containing frequencies of earthquake ground motions. The other purpose of an isolation system is to provide a mechanism for energy dissipation and to reduce the transmitted accelerations to the superstructure. In other words, by using base-isolation devices at the foundation of a structure, the structure is essentially decoupled from ground motion during earthquakes.

One type of seismic isolation systems currently being considered for nuclear facilities is the laminated elastomer bearing that uses high-damping elastomer layered between metallic plates (shims). This design is attractive because it combines the restoring and dissipating functions of an isolator into one compact, maintenance-free unit.

In order to produce an effective seismic isolation system and an efficient tool for analyzing the isolated structure, a design and analysis program of isolated structure is being established at Argonne National Laboratory (ANL). The detailed objectives of this program are: (1) to develop a material research and quality control program to characterize the large strain viscoelastic response of selected elastomers as well as to assure that the manufactured bearings meet the design specification, and (2) to develop three-dimensional computer codes to evaluate detailed isolator characteristics and the response of various isolated structure systems, including the effect of soil-structure interaction [2].

As part of the analytical development, a three-dimensional program SISEC (Seismic Isolation System Evaluation Code) is being developed at ANL for calculating the global response of isolators and isolated structures. The basic code utilizes beam, nonlinear spring and plate elements to model the isolated structure together with an elastic half space approach to evaluate the impedance functions of the soil domain [2].

Recently significant improvements have been made to the SISEC code. First, to closely simulate the bearing behavior, a nonlinear viscoelastic constitutive model by Simo and Taylor [3-5] has been modified [6,7] and implemented into the SISEC code. This formulation requires six input parameters derived from sinusoidal experimental data. The characteristic behavior of the isolation bearing, such as the variation of shear modulus with maximum shear deformation and material damping, are captured rather closely by the formulation. In the constitutive model, the material degradation is affected by a function which depends on the Eulerian norm of the deviatoric strains. Volumetric strains are considered to be entirely elastic. The resultant analytical model simulates the bearing behavior rather realistically.

Secondly, since structural response also depends significantly on the input acceleration time histories acting on the foundation level, a soil analysis is performed first to evaluate the foundation input motion as well as the stiffness and damping of the soil deposits. The analysis further accounts for isolator non-linearities, foundation embedment, inertia and kinematic interactions between the soil and structure.

In this paper, analytical developments of high damping elastomer bearings and improved soil structure interaction model are briefly described. The constitutive model was validated first against experimental data of PRISM bearing. System response analyses of based-isolated

structures are carried out with the time history method. Relative response of isolated and unisolated structures are also investigated.

## 2. ANALYTICAL DEVELOPMENTS

### 2.1 Nonlinear Viscoelastic Constitutive Model

The constitutive relation for viscoelastic material usually involve the deformation gradient denoted by **F**. This is a matrix which arises when the spatial coordinates are differentiated with respect to the material coordinates. By polar decomposition the deformation gradient in turn can be directly related to the right Cauchy-Green tensor **C** as follows:

$$\mathbf{C} = \mathbf{F}^T\mathbf{F} , \tag{1}$$

where the superscript T designates the transpose of a matrix. This tensor, also called the right stretch tensor, measures pure deformation. It also reduces to a unit matrix in the undeformed state. Similarly, the volume-preserving right Cauchy-Green tensor is given as

$$\bar{\mathbf{C}} = \mathbf{C}J^{-2/3} , \tag{2}$$

where J is the determinant of **F** (or det **F**).

In the viscoelastic constitutive formulation proposed by Simo and Taylor [3,4,5] the volumetric response of the material is assumed to be purely elastic; the viscoelastic effects are embodied by the deviatoric component. Their formulation is related to the second Piola-Kirchhoff stress tensor $\sigma$. The basic constitutive model is expressed as a convolution integral of the form

$$\sigma(t) = K \ln J + \int_0^t \mu(t-s)\, \dot{\pi}[e(s),\varphi_t]\, ds \,, \tag{3}$$

where the first term on the right side of the equation represents the volumetric component of stress and the second term stands for the deviatoric component. The bulk modulus K and the determinant of **F** (or det **F**) finalize the volumetric expression of the stress formulation.

The deviatoric part is composed of non-linear functions of the strain deviator and the damage variable $\varphi_t$. Here the more conventional approach of strain rate is replaced by the rate of non-linear function of the strain. The term $\mu(t)$ is the relaxation function and $\pi[e(t),\varphi_t]$ is a non-linear function of the strain history and the damage variable $\varphi_t$. The relaxation function $\mu(t)$ is taken to be of conventional form as an exponential function

$$\mu(t) = G_\infty + (G_o - G_\infty)\, e^{-t/\nu} \,, \tag{4}$$

where $G_\infty$ and $G_o$ are the long-term and short-term shear moduli of the material, respectively; $\nu$ is the time constant and t is time. The first three parameters are determined from experimental data.

The strain history function can be expressed as a product of two other functions, one dependent $\varphi_t$ and the other on deviatoric strain and $\varphi_t$:

$$\pi[e(t),\varphi_t] = g(\varphi_t) \cdot \gamma[e(t),\varphi_t] \,, \tag{5}$$

where $g(\varphi_t)$ is referred to as the "loading function" and $\gamma[e(t),\varphi_t]$ is the "damage function". Both terms can be related to the physical behavior of the material. The loading function $g(\varphi_t)$ is analogous to that encountered in plasticity formulations, which has reference to limiting stress. In this context the $g(\varphi_t)$ function relates the experimental variation of storage and loss moduli of

the material with respect to the damage variable $\varphi_t$. Simo and Taylor found that $g(\varphi_t)$ could be represented by

$$g(\varphi_t) = \varphi_t\left[\beta + (1-\beta)\,\frac{1-e^{-\varphi_t/\alpha}}{\varphi_t/\alpha}\right], \tag{6}$$

where $\alpha$ and $\beta$ are input parameters and can be referred to as the damage exponent and damage limit, respectively. The derivative of this function with respect to the damage parameter in turn represents the variation of the moduli as derived from experimental data.

The strain history damage function $\gamma[e(t),\varphi_t]$ must satisfy the conditions as

$$||\gamma[e(t),\varphi_t]|| = 1 \quad \text{iff} \quad ||e(t)|| \equiv \varphi_t ,$$

$$\text{tr}\{\gamma[e(t),\varphi_t]\} \equiv 0 , \tag{7}$$

$$\gamma[e(t),\varphi_t]\big|_{\varphi_{t=0}} = 0 .$$

The simplest function which satisfies all the above conditions is

$$\gamma[e(t),\varphi_t] = \frac{e(t)}{\varphi_t} \tag{8}$$

The product of the selected functions $g(\varphi_t)$ and $\gamma[e(t),\varphi_t]$ terms make up the history function representing the degradation of the material.

The integral expression of the deviatoric part can then be related to the following stress integral

$$\sigma(t) = K \ln J + \int_0^t \mu(t-s)\ \dot{\pi}(s)\ ds\ , \tag{9}$$

where $\pi(s)$ is a deviatoric "effective" Lagrangian strain defined as follows:

$$\pi(s) = \left[\beta + (1-\beta)\ \frac{1-e^{-\varphi_s/\alpha}}{\varphi_s/\alpha}\right] \mathrm{dev}\bar{C}(s)\ , \tag{10}$$

and $\varphi_s$ can also be expressed in terms of the same variables, i.e.,

$$\varphi_s = \max||\mathrm{dev}\bar{C}(s)||\ . \tag{11}$$

In physical terms $\varphi_s$ is simply the maximum value attained by the norm of $\mathrm{dev}\bar{C}(s)$ during the past history of loading.

In order to numerically integrate the constitutive equation, it is convenient to evaluate the convolution integral through a recurrence relation. By employing a generalized mid-point rule and the mean value theorem the following algorithm results for calculating the Cauchy stress $\tau_{n+1}$ which with minor modifications is taken from Refs. [3-5]. Thus, starting from the deformation gradient $F_{n+1}$:

$$C_{n+1} = F_{n+1}^T\ F_{n+1}\ ,$$

$$\bar{C}_{n+1} = C_{n+1}\ J_{n+1}^{-2/3}\ ,\ \text{where}\ J_{n+1} = \det F_{n+1} \tag{12}$$

$$||\mathrm{dev}\bar{C}_{n+1}|| = \left\{\mathrm{dev}\bar{C}_{n+1} \cdot \left[\mathrm{dev}\bar{C}_{n+1}\right]^{T}\right\} ,$$

$$\varphi_{n+1} = \max\left\{||\mathrm{dev}\bar{C}_{n+1}||, \varphi_{n}\right\} ,$$

$$\pi_{n+1} = \left[\beta + (1-\beta)\,\frac{1-e^{\varphi_{n+1}/\alpha}}{\varphi_{n+1}/\alpha}\right] \mathrm{dev}\bar{C}_{n+1} ,$$

$$\Delta\pi_{n+1} = \pi_{n+1} - \pi_{n} ,$$

$$\Delta h_{n+1} = \left(e^{-\Delta t/v} - 1\right)\left[h_{n} - \frac{G_{o} - G_{\infty}}{\Delta t/v}\,\Delta\pi_{n+1}\right] , \qquad \text{(12 Cont'd)}$$

$$h_{n+1} = h_{n} + \Delta h_{n+1} ,$$

$$\sigma_{n+1} = \sigma_{n} + K\,\Delta\ln J_{n+1} + \Delta h_{n+1} + G_{\infty}\Delta\pi_{n+1} ,$$

$$\tau_{n+1} = \left(\det F_{n+1}\right)^{-1} F_{n+1}\sigma_{n+1}F_{n+1}^{T} .$$

The last expression converts the second Piola-Kirchhoff stress to the Cauchy stress. It is observed that if the constitutive relation is devoted to pure (or simple shear) then certain simplifications apply. Specifically, the volumetric component does not need to be calculated, for it is set to be zero. Furthermore, the second Piola-Kirchhoff stress then will accurately represent the stress and the last step of the algorithm table need not be calculated.

The original Simo-Taylor (S-T) constitutive model [3-5] can rheologically be represented by a series combination of a damper and a non-linear spring, similar to the conventional Maxwell chain model. The damping pertains to the effect of the relaxation function with the time parameter and the variable resistance is associated with the non-linear shear modulus. In the modified S-T relation the original S-T model is set in parallel with another non-linear resistance of the S-T model as shown in Fig. 1. The weight ratio of the original S-T model to the non-linear resistance is the sixth parameter C required as input. This modified S-T constitutive relation was found to possess certain advantages in the representation of the bearings in shear.

The derivation of the input parameters can best be accomplished by means of a short computer program especially written for that purpose. Two ($\alpha$,$\beta$) out of the six parameters are derived from experimental plots of the storage and loss moduli. These moduli are derived in the process of normalizing both plots onto a single fit. The next two parameters ($G_0$ and $G_\infty$) are the shear stiffness at very small strain and the stiffness at very large strain; they are read off from an experimentally derived plot showing the variation of shear stiffness with maximum strain.

The remaining two constants (the so-called time parameter $\nu$ and C parameter) are best derived by the above-mentioned simple computer program. These two parameters are varied as input in the program to reproduce the experimentally recorded hysteresis loops of the bearing material. The computer program analytically subjects the material coupon to sinusoidal displacement and calculates the corresponding stress. The results are plotted in the form of hysteresis loops. The values of time parameter $\nu$ and C constant are properly determined when the resulting hysteresis loops correspond to those derived experimentally. Naturally, the most

important factor in the proper matching is the area within the hysteresis loop, which is the measure of material damping.

## 2.2 Soil-Structure Interaction

Since a base-isolated structure may have a highly nonlinear rubber bearing at its base and its foundation is embedded in a layered soil deposit, the suitable soil-structure interaction (SSI) analysis should be able to capture these important factors. Here, a three-step spring method [8] is adapted for the soil analysis. This method is illustrated in Fig. 2. Briefly, it consists of three major steps. The first step calculates the foundation input motions (translation and rotation) from the site specific free-field motion. The calculation is based on the theory of elastic wave propagation in combination with the assumption that the motion is composed of the vertically propagating body waves. The second step evaluates the impedance functions for the embedded foundation. The third step is using the foundation input motion and impedance function as input to the SISEC code to perform the detailed SSI analysis.

Due to the foundation embedment and the inability of the rigid foundation to conform to the free-field motion, the foundation experiences not only the horizontal translation motion but also the rocking motion for a purely horizontal free-field motion. These horizontal and rocking motions, denoted by $X_i(t)$ and $\varphi_i(t)$, respectively, are obtained by applying the transfer functions [8] to the free-field motion and are given by:

$$\ddot{X}_i(t) = \mathrm{IFT}\begin{cases} \ddot{X}_g(\omega)\left[\cos\left(\frac{\pi}{2}\,\frac{f}{f_n}\right)\right] & \text{if } f \le 0.7\ f_n \\ \ddot{X}_g(\omega)[0.453] & \text{if } f > 0.7\ f_n \end{cases} \tag{13}$$

and (13)

$$\ddot{\phi}_i(t) = \mathrm{IFT}\begin{cases} \ddot{X}_g(\omega)\left[0.257\left(1 - \cos\frac{\pi}{2}\frac{f}{f_n}\right)/R\right] & \text{if } f \le 0.7\ f_n \\ \ddot{X}_g(\omega)[0.257/R] & \text{if } f > 0.7\ f_n \end{cases}$$

where IFT stands for Inverse Fourier Transformation; $X_g(\omega)$ is the Fourier transform of the horizontal acceleration at the free surface in the free field, and $f_n$ is the fundamental shear frequency of the embedment region. Here the descrete Fourier transformation and the fast Fourier transformation algorithms are employed to compute the foundation input motions.

To evaluate the impedance functions we assume the structural foundation is embedded in a homogeneous stratum. Let F and M be the horizontal force and rocking moment at the interface of the foundation and soil, X and $\phi$ be the corresponding lateral and rocking displacements, the force-displacement relationship can be written as

$$\begin{Bmatrix} F \\ M \end{Bmatrix} = \begin{bmatrix} K_{xx} & K_{x\phi} \\ K_{x\phi} & K_{\phi\phi} \end{bmatrix} \begin{Bmatrix} X \\ \phi \end{Bmatrix} \tag{14}$$

where $K_{xx}$ $K_{x\phi}$, and $K_{\phi\phi}$ are the impedance functions. In frequency domain, these functions are conveniently expressed in the following form:

$$K_{xx} = K_{xx}^0(k_{11} + ia_0c_{11})(1 + 2i\beta)\ ,$$

$$K_{x\phi} = K_{x\phi}^0(k_{12} + ia_0c_{12})(1 + 2i\beta)\ , \tag{15}$$

$$K_{\phi\phi} = K^0_{\phi\phi}(k_{22} + a_0 C_{22})(1 + 2i\beta)$$

in which $a_0$ = a dimensionless frequency parameter defined by

$$a_0 = \frac{\omega R}{V_s} \tag{16}$$

and $V_s$ is the shear wave velocity of the soil deposit [8]. In general, $K^0_{xx}$, $K^0_{\phi\phi}$ are functions of the soil shear modulus, radius of the foundation, depth of the embedment, and the depth of bedrock, soil Poisson's Ratio, etc.; the damping coefficients $C_{11}$, $C_{12}$, and $C_{22}$ depend on the hysteretic damping of soil, the soil dilational wave velocity, and fundamental shear and dilatation frequencies of the stratum. For detailed expressions of these stiffness and damping coefficients one should refer to Ref. [8].

## 3. Results and Discussions

### 3.1 Validation of Viscoelastic Constitutive Equation

A 1/4-scale test of an elastomeric bearing was performed by Professor J. M. Kelly at the Earthquake Engineering Research Center (EERC), University of California-Berkeley for the PRISM Liquid Metal Reactor Project [9-11]. In the test a sinusoidal shear loading is applied at the top of the isolator. A typical experimental hysteresis loop of the 1/4-scale bearing is shown in Fig. 3. Numerical simulation of the scale model test was accomplished by running a one-element problem within the SISEC environment. The hysteresis loops of analytical model due

to pure sinusoidal input is given in Fig. 4. As can be seen, the agreement of force-displacement relationships between the experimental and analytical results is quite good.

3.2 Response Analysis of Unisolated and Isolated Structures Under Horizontal Excitation

The finite-element model of a nuclear island is shown in Fig. 5. Two lumped-mass sticks are used to model the reactor containment and reactor building, respectively. In this model, the reactor containment is approximated by twelve (12) nodes interconnected by eleven (11) beam elements. The reactor building is discretized into eleven (11) nodes connected by ten (10) beam elements. The mass of the major components such as the reactor vessel is appropriately added to its associated nodes. Two calculations are performed dealing with unisolated and isolated plants, respectively. For the unisolated plant, one foundation mat is utilized. On the other hand, the isolated plant has two concrete foundation mats, and the isolators are placed between these two mats. The design fundamental frequency of the isolators is 0.50 Hz.

For calculation of the base-isolation structure, certain modeling techniques are required. In this calculation, beam elements are used for the super-structures. The isolators are modeled by two spring elements, one linear spring for simulating the large vertical stiffness and one nonlinear viscoelastic spring for modeling the relatively low stiffness in the horizontal direction. Thus, the vertical load-carrying capacity and necessary horizontal flexibility are appropriately modeled. The input to the horizontal nonlinear spring using the viscoelastic constitutive model was based on experimental data of 1/4-scale PRISM-type bearings given in the previous example whose hysteresis curve is shown in Fig. 3. The plot of bearing shear stiffness variations with maximum displacement (given in Fig. 6) was also utilized for determining the input values. The resulting input parameters required to generate the experimental curves are

$$G_0 = 250,\ G_\infty = 55,\ \nu = 0.35,\ \alpha = 0.10,\ \beta = 0.30,\ C = 0.55.$$

The area of the full-size PRISM bearing is 2124 $in^2$. A total of six hundred bearings is assumed for this illustration. For simplification of the analysis, only one composite isolator is used. This isolator represents the global effect of the estimated 600 isolators required for the frequency of 0.50 Hz. The free-field artificial input acceleration history and its Fast Fourier Transform (FFT) shown in Fig. 7 is used for the numerical analyses which has a peak ground acceleration of 0.20 g.

The horizontal acceleration time histories of node 1 (basemat), 23 (top of containment), and 43 (top of the reactor building) for the case of the unisolated structure are of special interest for studying the relative merits of the base-isolation system. Without the isolators, large accelerations are found, particularly at the top of the containment as illustrated in Fig. 8. The maximum accelerations at these three locations have values of 0.22 g, 0.43 g, and 0.33 g. The amplification factors at both the top of the containment and reactor building are 1.95 and 1.5, respectively.

For the case of isolated structures, we have found that the accelerations at nodes 1 (upper basemat), 23 (top of containment), and 43 (top of reactor building) have the similar response shape but smaller peak values. The maximum response accelerations at these three locations are about 0.083 g, 0.0875 g, and 0.085 g, respectively. Note that because of the lower frequency and softness of the isolator bearings in response to the horizontal excitation, the peak accelerations at these three locations are much smaller than that of the input ground acceleration which has a value of 0.20 g. In other words, by using the high damping elastomeric bearings the

superstructure is basically decoupled from the ground motion during the earthquake. For illustration, the acceleration history at node 43 (top of the reactor building) is given in Fig. 9 where the dominant frequency is about 0.50 Hz.

Figure 10 shows the plot of relative displacement of the bearing under the imposed seismic excitation. The maximum displacement is about 3.68 in. Figure 11 displays the corresponding force-displacement hysteresis plots of the composite bearing. The energy absorbed by the bearing is shown in Fig. 12.

Acknowledgement

This work was performed in the Engineering Mechanics Program of the Reactor Engineering Division of Argonne National Laboratory under the auspices of the U.S. Department of Energy, Contract No. W-31-109-Eng-38.

References

1. J. M. Kelly, "Recent Developments in Seismic Isolation," in Seismic Engineering: Recent Advances in Design, Analysis, Testing and Qualification Methods, pp. 381-386, 1987, ASME Pressure Vessel and Piping Conference, San Diego, CA, July 1987.

2. R. F. Kulak and C. Y. Wang, "Design and Analysis of Seismically Isolated Structures," Post Conference Seminar of the 10th Intl. Conf. on Structural Mechanics in Reactor Technology (SMiRT-10), Proc. 1st Intl. Seminar on Seismic Base Isolation for Nuclear Power Facilities, CONF-8908221, pp. 341-368, San Francisco, CA, August 21-22, 1989.

3. T. C. Simo and R. L. Taylor, "A Simple Three-Dimensional Viscoelastic Model Accounting for Damage Effects," Report No. UCB/SESM/83-10, SESM, U.S. Berkeley, 1983.

4. T. C. Simo and F. L. Taylor, "A Three-Dimensional Finite Deformation Viscoelastic Model Accounting for Damage Effects," Report No. UCB/SESM/85-02, SESM, U.C. Berkeley, 1985.

5. T. C. Simo, "On a Fully Three-Dimensional Finite-Strain Viscoelastic Damage Model: Formulation and Computational Aspects," Comput. Meths. Appl. Mech. Engrg. 60, pp. 153-173, 1987.

6. M. J. Kim, A. Gupta, and A. H. Marchertas, "Implementation of a 3-D Viscoelastic Material Model," Northern Illinois University Report NIU/ME 89/01, September 1990.

7. R. F. Kulak and A. H. Marchertas, private communication, July 1990.

8. E. Kausel, R. V. Whitman, J. P. Morray and F. Elsabee, "The Spring Method for Embedded Foundations," Nucl. Eng. & Design, Vol. 48, pp. 377-392, 1978.

9. J. M. Kelly and M. Celebi, "Verification Testing of Prototype Bearings for a Based Isolated Bearing," Report No. UCB/SESM-84/01, SESM, U.S. Berkeley, 1984.

10. R. F. Kulal, personal communication, Argonne National Laboratory, September 1989.

11. F. F. Tajirian and T. M. Kelly, "Testing of Seismic Isolation Bearings for Advanced Liquid Metal Reactor Prism," in Seismic, Shock, and Vibration Isolation - 1988, Edited by H. Chung and N. Mostaghel, ASME Publication, PVP - Vol. 147, 1988.

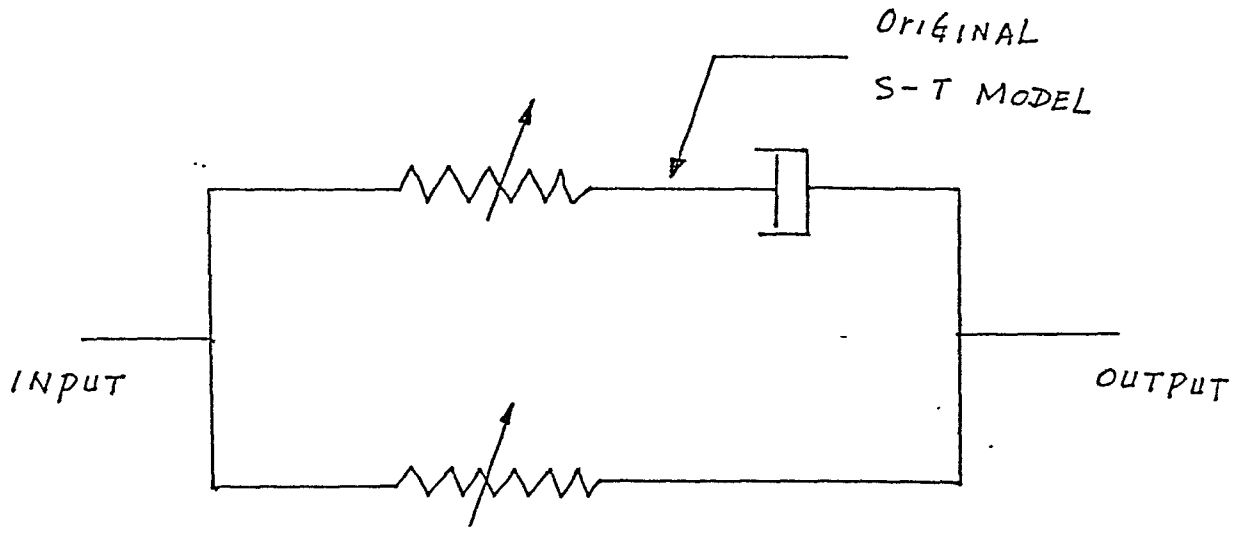


Fig. 1. Modified S-T Constitutive Model

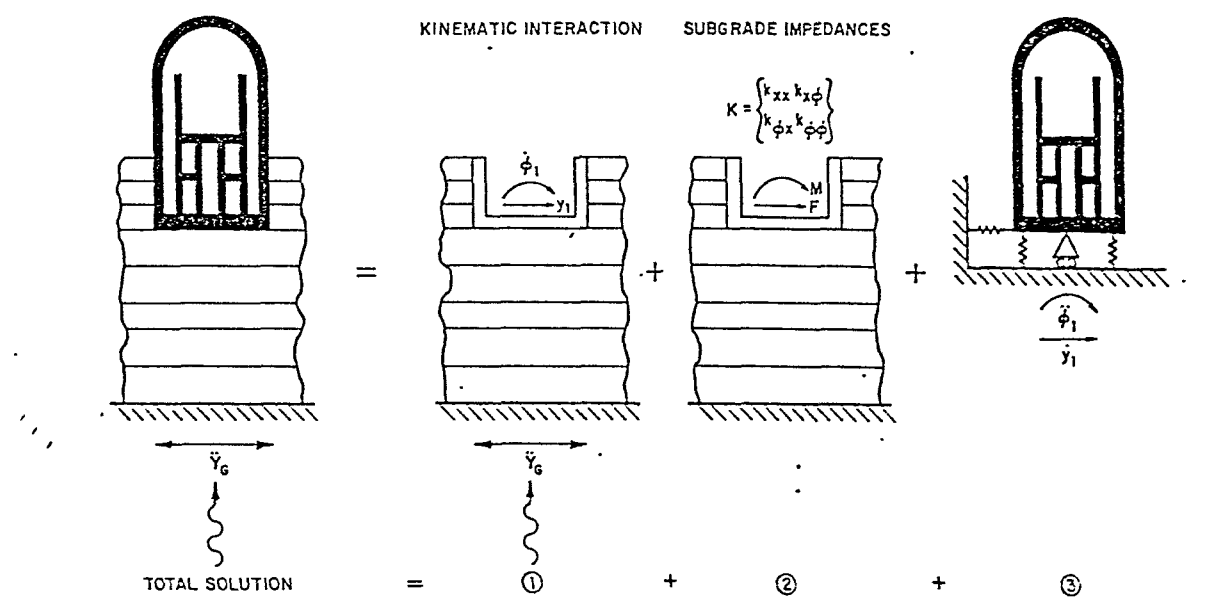


Fig. 2. Three-Step Spring Method for Soil-Structure Interaction Analysis

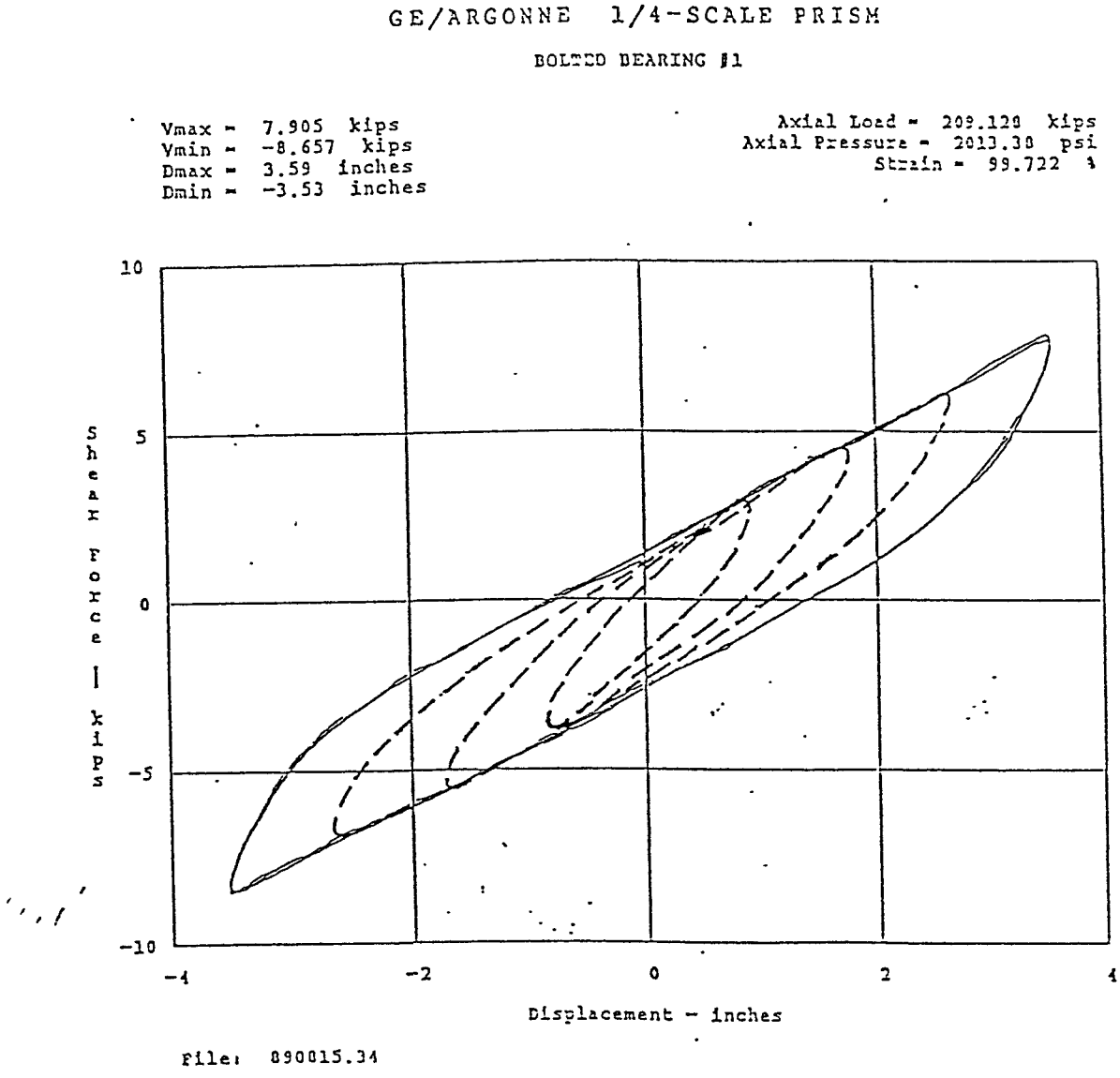


Fig. 3. Typical Hysteresis Loop of a 1/4-Scale PRISM Bearing

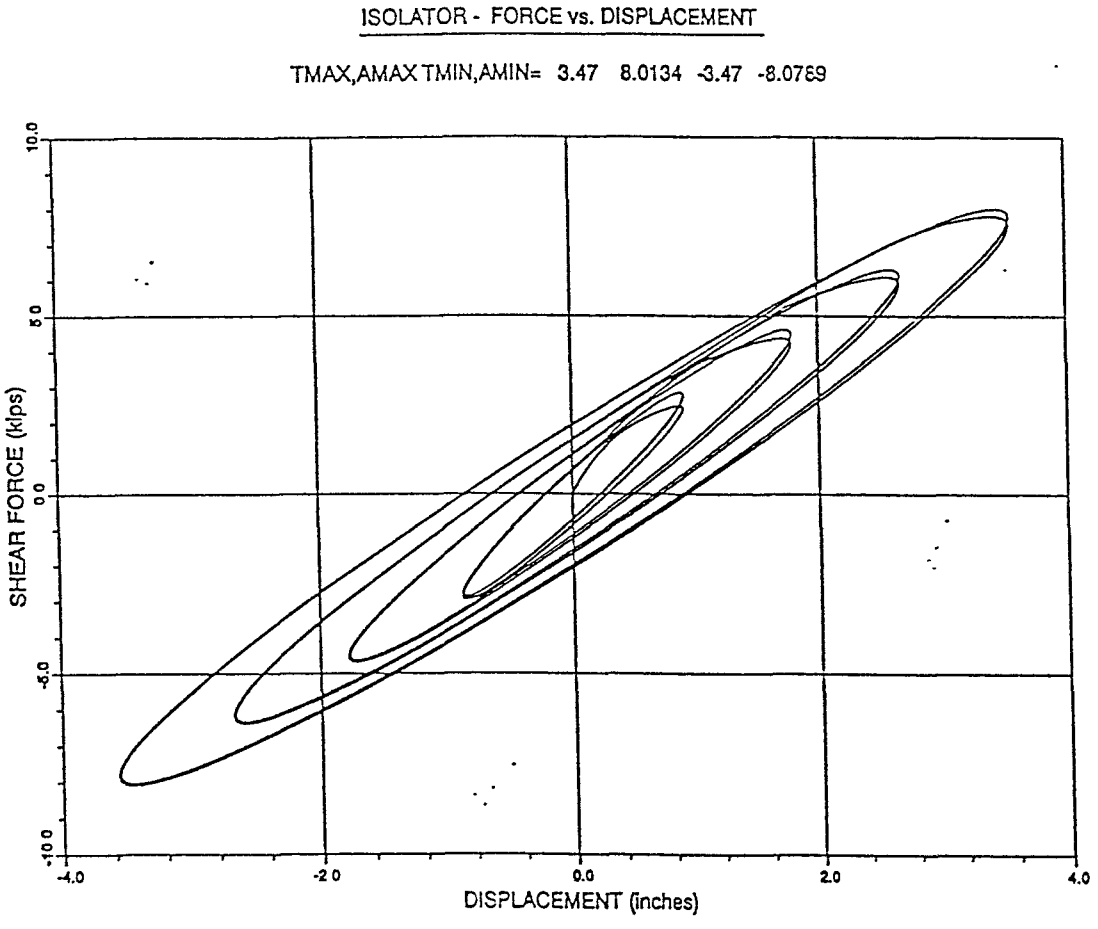


Fig. 4. Hysteresis Loops of Analytical Model

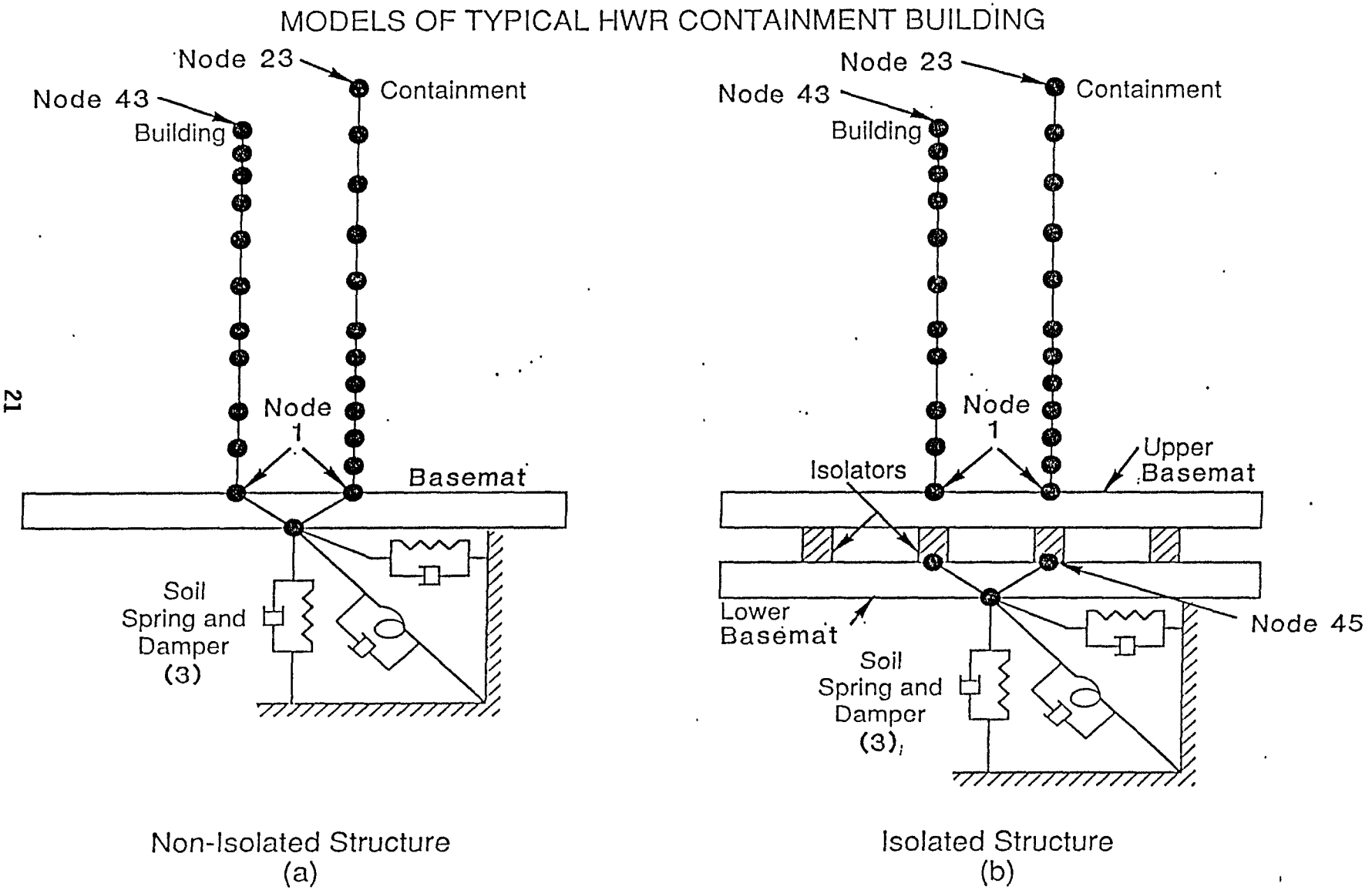


Fig. 5. Finite-Element Model of a Nuclear Island

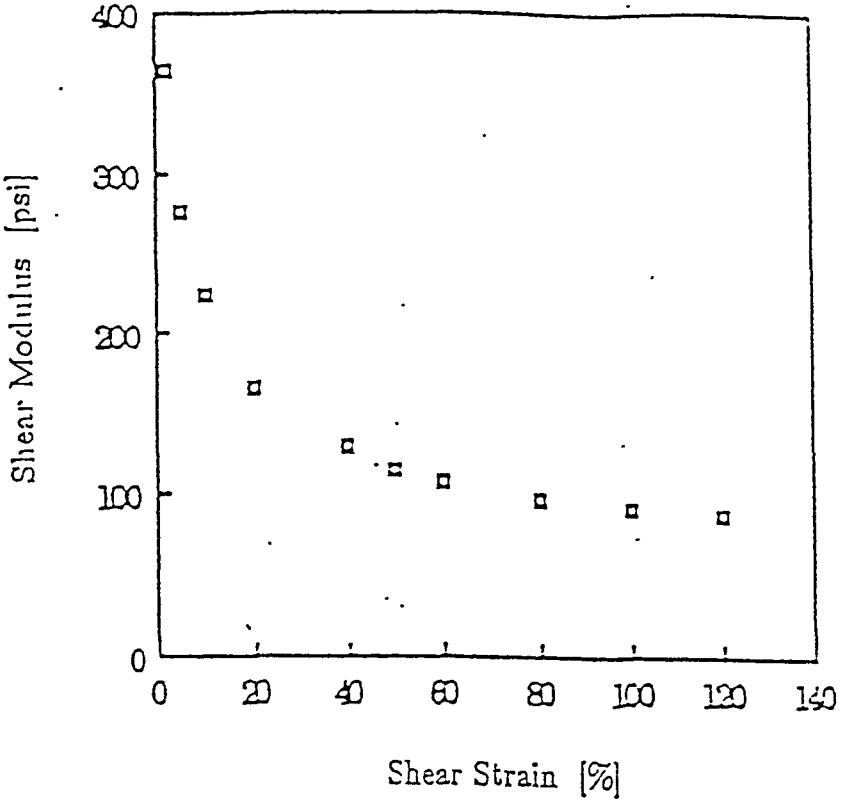


Fig. 6. Variation of High-Damping Elastomer Shear Modulus with Shear Strain

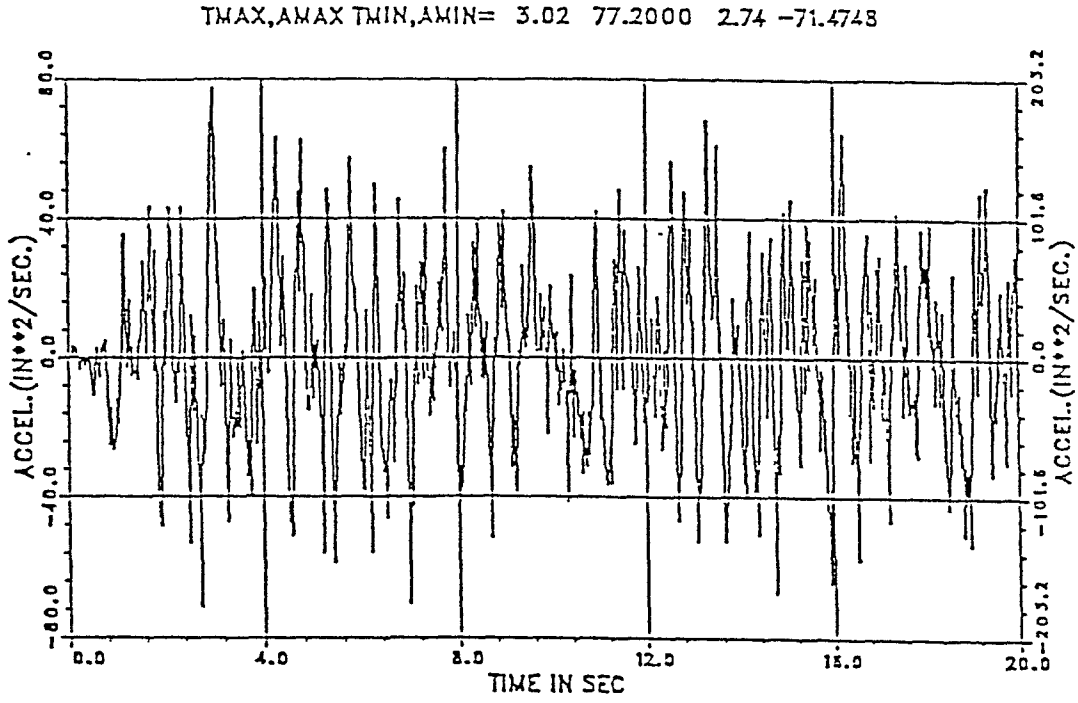


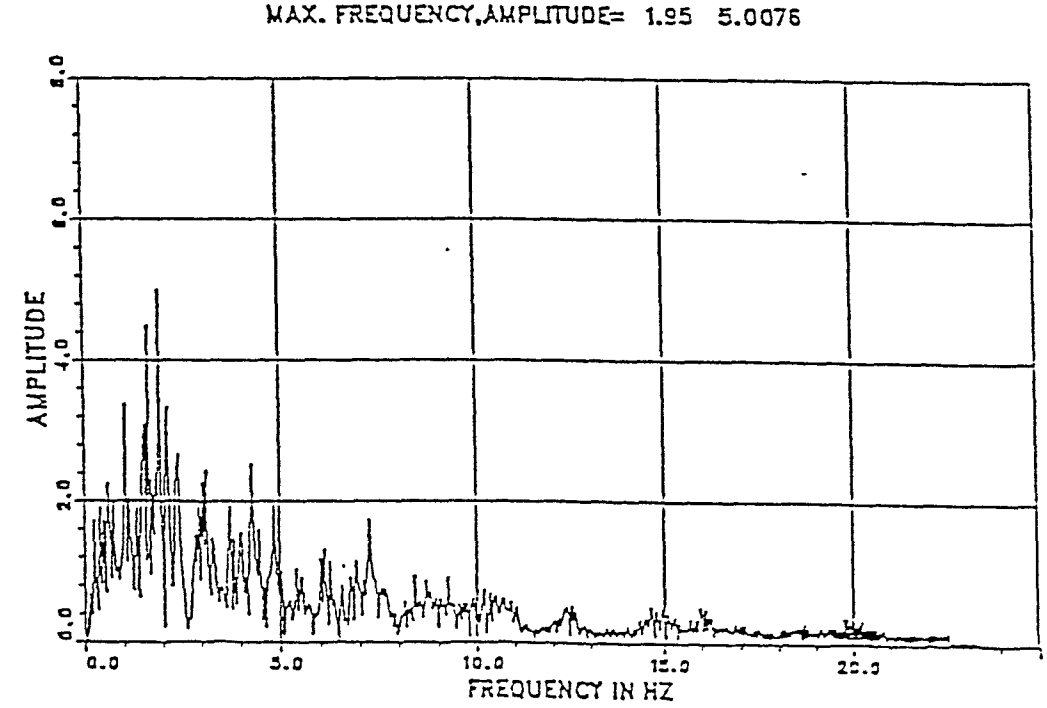


Fig. 7. The Input Free Field Artificial Acceleration History for Simulating the Horizontal Excitation

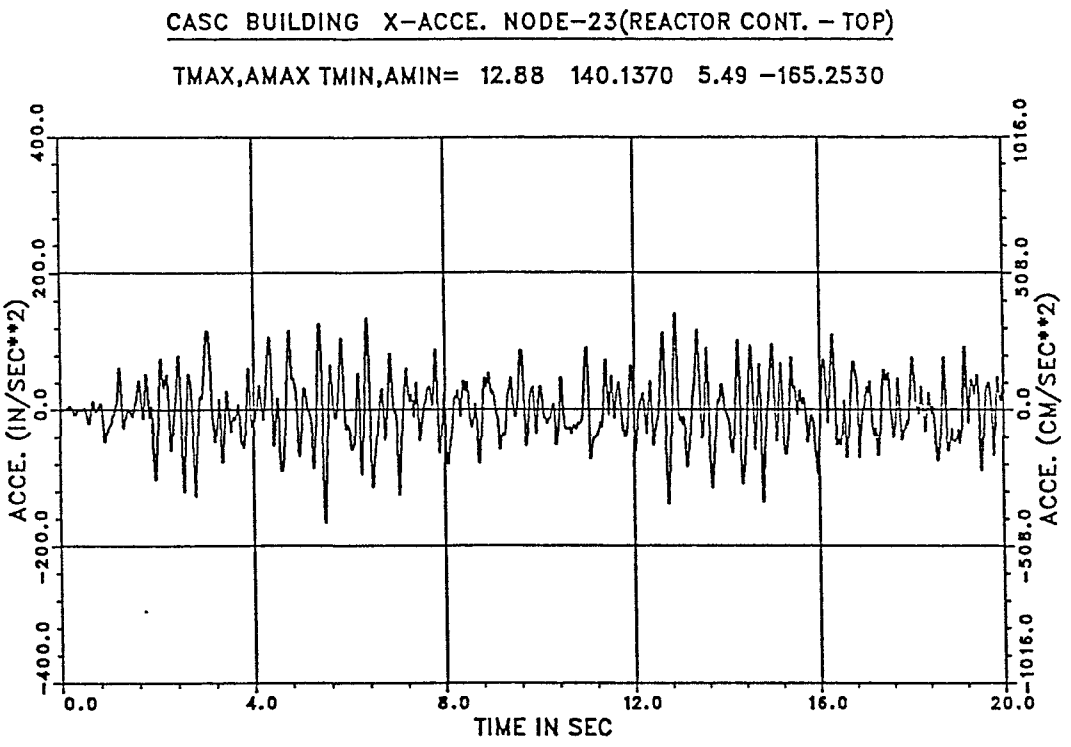


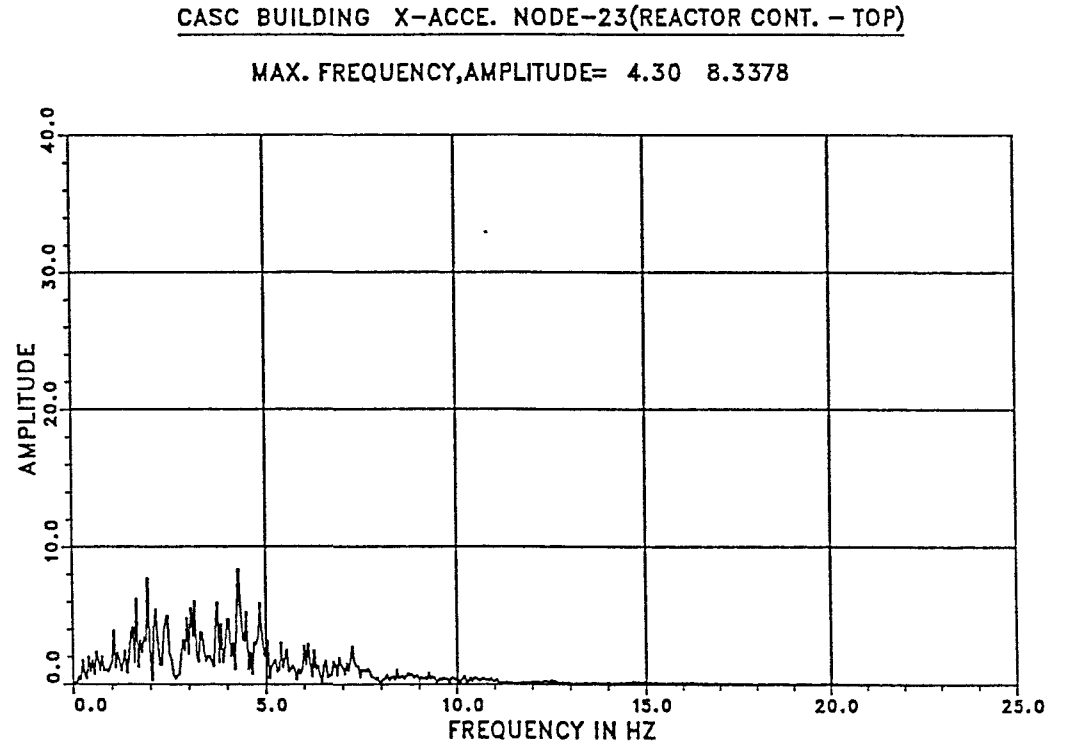


Fig. 8. Horizontal Acceleration History and its FFT at the Top of the Containment of a Unisolated Structure

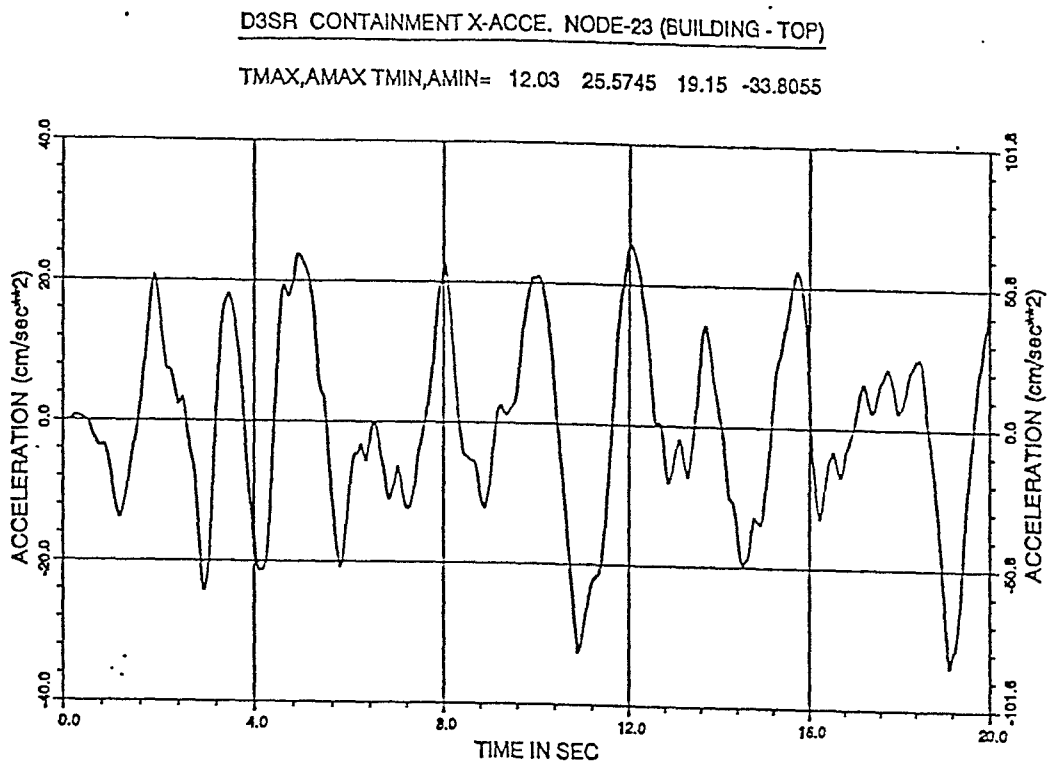


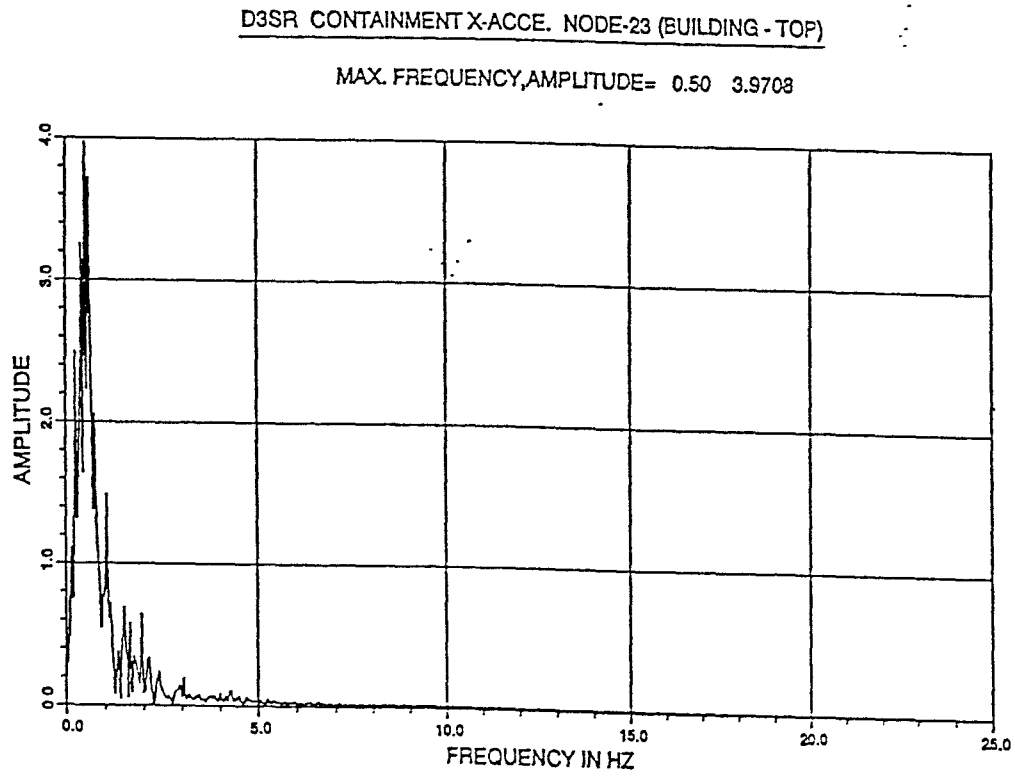


Fig. 9. Horizontal Acceleration History and its FFT at the Top of the Containment of a Isolated Structure

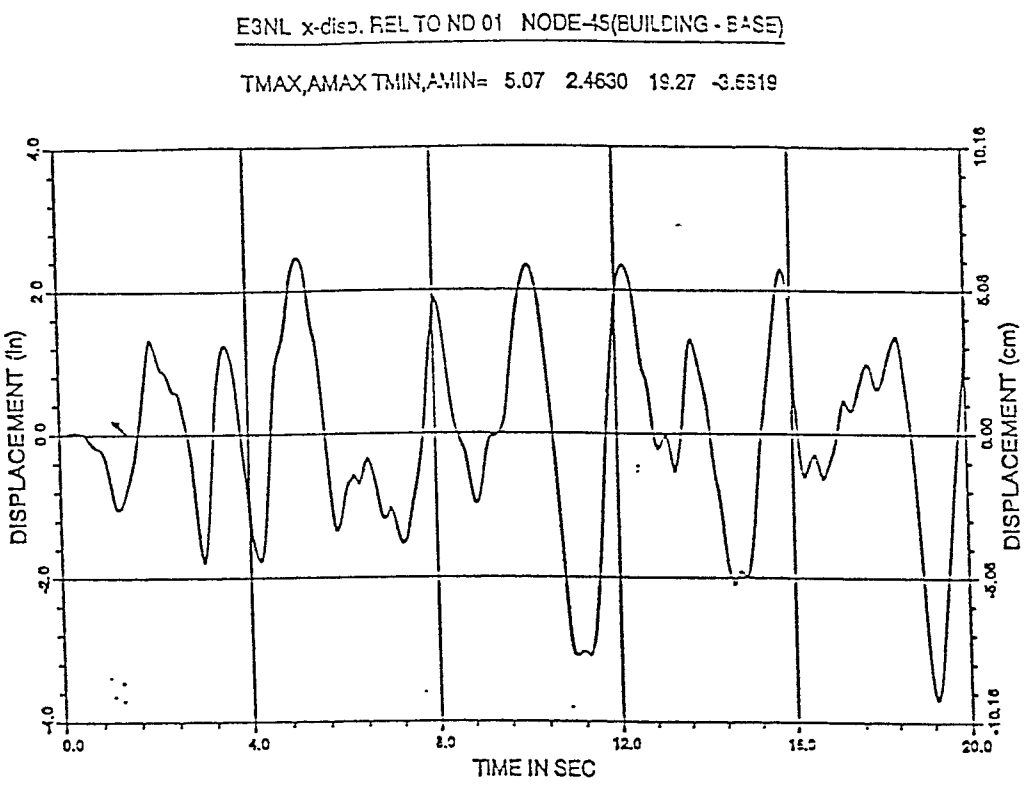


Fig. 10. Relative Displacement of the Elastomer Bearing

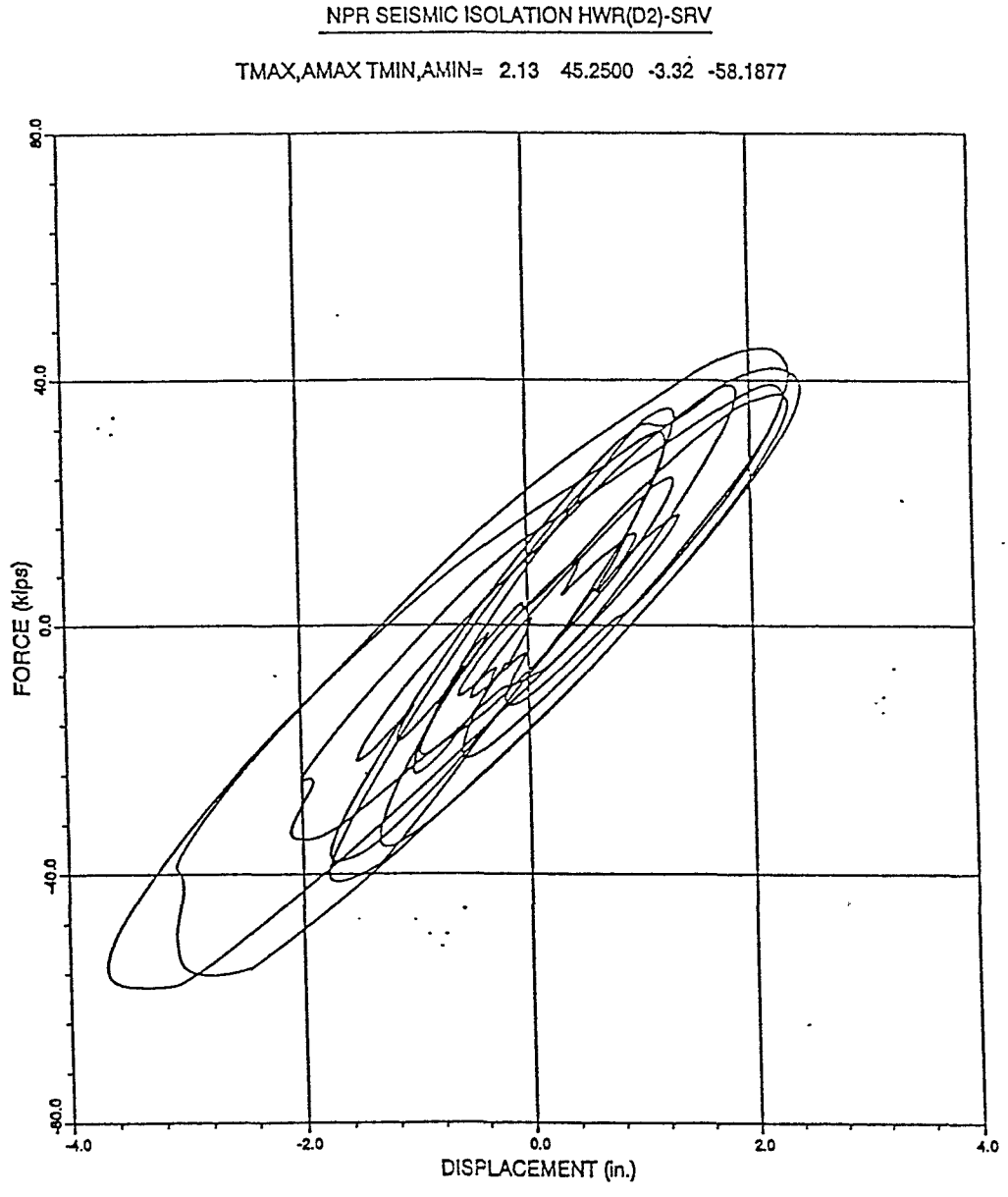


Fig. 11. Force-Displacement Hysteresis Loops of the Composite Bearing

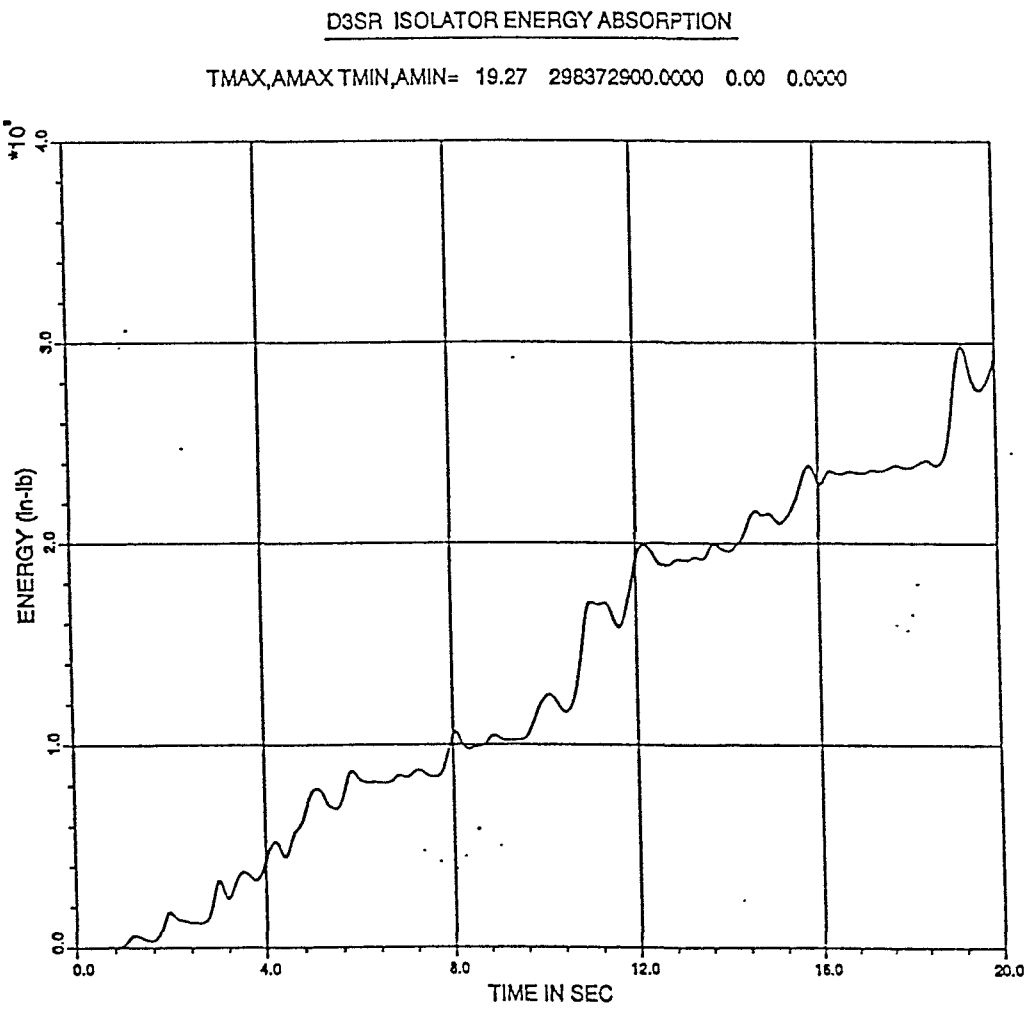


Fig. 12. Energy Absorbed by the Bearing